

## SUPPLEMENTARY INFORMATION

## Supplementary Results

### Auxin effect on endocytosis and PIN polarity

Auxin has been shown to inhibit endocytosis including internalization of PIN proteins<sup>1</sup>. Therefore we tested whether this auxin effect has impact on PIN polarization. We observed that in presence of exogenous application of auxin, PIN1-YFP polarization following photobleaching was visibly delayed (Supplementary Fig. 2a, b) as compared to untreated controls (Figure 1a, b). In addition, we tested importance of auxin-regulated endocytosis for PIN polar localization under steady-state conditions. We compared PIN1 polarity in cells with different cellular auxin levels as indirectly inferred from the activity of auxin responsive reporter *DR5rev::ER-GFP*<sup>2</sup>. In *Arabidopsis* root, cells within the DR5 maximum such as in quiescent centre and columella show less polar PIN signal<sup>3,4</sup>. Notably, some central cell files of the stele such as protophloem<sup>5</sup> or protoxylem<sup>6</sup> show elevated DR5 activity which correlates with less pronounced polar PIN1 localization as compared to the adjacent cell files with lower DR5 activity (Supplementary Fig. 2h). Thus it seems that elevated cellular auxin levels often correlate with decreased polarity of PIN localization in these cells.

To further substantiate the relation between auxin-dependent inhibition of endocytosis and PIN polarity, we performed temporal manipulation of auxin levels in combination with quantitative analysis of PIN polarity in lateral root cap cells. We expressed PIN2-GFP under the control of auxin-insensitive lateral root-cap specific promoter and manipulated auxin levels by (i) pharmacological inhibition of auxin efflux, (ii) exogenous application of auxin and by (iii) ectopic overexpression of bacterial auxin biosynthetic enzyme IAAH under the control of WOX5 promoter<sup>4,7</sup> which allows induction of auxin biosynthesis in the quiescent centre by external addition of the precursor IAM<sup>8</sup> and its rapid polar translocation towards the lateral root cap cells<sup>4</sup>. In all three cases, increase in auxin levels leads to less polar PIN localization (Supplementary Fig. 2c-g). This further substantiate that auxin-based inhibition of endocytosis interferes with effective PIN polarization.

The developmental role of the endocytosis-based modulation of PIN polarity is unclear but it might be related to rapid changes of PIN polarity towards the auxin maxima as observed for example during phylotactic initiation of leaves and flowers<sup>9-11</sup>. This

mechanism is probably distinct from the auxin-dependent PIN polarization away from the auxin maxima as observed during formation and regeneration of vascular tissue<sup>12,13</sup>.

### Characterization of *Arabidopsis* Rab5 endocytic pathway mutants

Rab5 is one of the best studied regulators of endocytosis in mammalian cells. In mammalian cells it localizes to early endosomes and regulates early endocytic steps at the plasma membrane (PM)<sup>14-19</sup>. Rab5 acts as molecular switch by cycling between the GDP-bound inactive and GTP-bound active states<sup>20</sup>. Rab5 is activated by the guanine nucleotide exchange factor (GEF) that stimulates release of GDP and allows binding of the GTP<sup>21</sup>. In contrast, Rab5 is inactivated by GTPase-activating protein (GAP) that accelerates GTP hydrolysis<sup>22</sup>. The GDP-bound (inactivated) form of Rab5 is released from the membrane and remains in the cytosol. In mammalian cells dominant negative (DN) mutant of Rab5 (GDP-locked Rab5) inhibits endocytosis whereas dominant active (DA) Rab5 (GTP-locked Rab5) mutant accelerates endocytosis suggesting the rate limiting effect of Rab5 activity on endocytosis<sup>14,18,23</sup>.

The *Arabidopsis* genome contains two conventional Rab5 homologues Ara7 (At4g19640) and Rha1 (At5g45130) that localize to endosomes<sup>24</sup>. Therefore to understand the role of Rab5 pathway in plants, hereby, we characterized loss-of-function mutants of Ara7 and Rha1 and created the double *ara7rha1* mutant (Supplementary Fig. 3a, b). Based on expression analysis, *ara7* is a full knockout and *rha1* is a leaky mutant (Supplementary Fig. 3b). *ara7* and *rha1* does not exhibit noticeable phenotypic defects (Supplementary Fig. 3c), whereas *ara7rha1* double mutant is gametophytic lethal (not shown). This demonstrates the redundant and essential role of Rab5 homologues in plants, however it does not allow further characterization of the role of Rab5 pathway by this approach. We thus sought for another way to interfere with Rab5-dependent processes. Activation of Rab5 is mediated by GDP-GTP exchange factor (GEF) and Rab5 GEF contains a highly conserved and Rab5-specific VPS9 domain that catalyses exchange of GDP to GTP on Rab5 in mammalian and yeast cells<sup>15,25</sup>. We found one expressed protein containing the VPS9 domain in *Arabidopsis* [which we refer to as AtVps9a (At3g19770)] that activates both Ara7 and Rha1 *in vitro* by physically interacting with them<sup>26</sup>. In this study we analyzed two alleles of *atvps9a* (called as *atvps9a-1* and *atvps9a-2*) in detail

(Supplementary Fig. 3a-c). *atvps9a-1* has T-DNA insertion upstream of VPS9 domain and thus it is a full knockout. Accordingly, *atvps9a-1* is embryo lethal<sup>26</sup>; whereas in another allele *atvps9a-2*, T-DNA is inserted after the VPS9 domain and based on RT-PCR analysis it is a leaky allele (Supplementary Fig. 3a, b). However, *atvps9a-2* still displays clear phenotypic defects such as reduced growth (Supplementary Fig. 3c).

Another way to interfere with Rab5 function is to use overexpression of GDP-locked (DN) version of Rab5, which impairs endocytosis in mammalian cells<sup>14,18</sup> and has been used to impair endocytosis in plants<sup>27</sup>. Therefore, we expressed DN form of Ara7 in *Arabidopsis* plants using a tamoxifen-inducible *UAS::GAL4* based trans-activation system<sup>28</sup>. We examined the cellular consequences of DN-Ara7 expression. After 3 hr induction, DN-Ara7 becomes cytosolic in contrast to a normal localization of Ara7 to endosomes (Supplementary Fig. 3d). Also in *atvps9a-1*, GFP-Ara7 remains cytosolic instead of localizing to endosomal compartments [Supplementary Fig. 3d]. These results fit with the paradigm from the animal field and show that AtVps9a-mediated activation of Ara7 is important for its normal endosomal localization and that locking Ara7 in an inactive, GDP-bound state prevents its localization to endosomes.

Next we generated AtVps9a-GFP fusion that fully complements the *atvps9a-1* mutant confirming that this chimeric protein is completely functional (Supplementary Fig. 3c). Then we examined the subcellular localization of AtVps9a. AtVps9a colocalizes with Ara7 (Supplementary Fig. 3e) consistent with the *in vitro* interaction results<sup>26</sup> and it also colocalizes with the endosomal compartments labelled by the endocytic tracer FM4-64 (Supplementary Fig. 3f). In *Arabidopsis*, Brefeldin A (BFA) inhibits recycling but not endocytosis by targeting the ARF-GEF GNOM and thus it induces aggregation of endosomes into so called ‘BFA compartments’<sup>29,30</sup>. Upon BFA treatment, FM4-64 labelled endosomal compartments and AtVps9a-GFP compartments co-aggregate into BFA compartments (Supplementary Fig. 3g). These results indicate that AtVps9a resides on endosomes and recruits Ara7 (and Rha1) to endosomes.

### Effect of Rab5 interference on endocytosis, recycling and various intracellular compartments

We analyzed effects of the interference with Rab5 pathway on endocytosis and other cellular processes. An established way to monitor endocytosis is to follow internalization of a fluorescent lipophylic dye FM4-64<sup>24,29,31</sup>. Both in *DN-Ara7* and in *atvps9a-2*, FM4-64 internalization is reduced indicating endocytic defects (Supplementary Fig. 4a). Next we analyzed PIN internalization in *DN-Ara7* and in *atvps9a-2*. BFA inhibits PIN recycling but allows endocytosis leading to PIN internalization<sup>30</sup>. In controls, BFA treatment induces formation of large PIN-labelled BFA compartments whereas in *DN-Ara7* and in *atvps9a-2*, less PIN is internalized as inferred from formation of smaller PIN-labelled BFA compartments (Supplementary Fig. 4b). We also tested whether BFA-monitored internalization of other cell surface-resident proteins is affected in case of interference with Rab5 pathway. We found that internalization of other PM proteins such as PM-ATPase (Supplementary Fig. 4c), aquaporin PIP1 (Supplementary Fig. 4f, g) and syntaxin NPSN12 (Supplementary Fig. 4d, e) is reduced in case of interference with Rab5 pathway. Thus interference with Rab5 pathway leads to impairment of endocytosis and reduced internalization of many PM-resident proteins including PINs.

Next we examined the effect of interference with Rab5 pathway on PIN1 recycling. Following BFA treatment, we washed out BFA under conditions of conditionally expressed *DN-Ara7*. In controls, the recycled PIN1 after BFA washout arrives first at the PM in a less polar manner and within 3 hrs attains its normal basal polarity (Supplementary Fig 5). On the other hand, after BFA washout with concomitant *DN-Ara7* expression, PIN1 shows normal rate of re-appearance at the PM but it sustains less polar distribution for a prolonged time (Supplementary Fig. 5). This indicates that impairment of Rab5 pathway does not block PIN recycling but interferes with PIN1 polarization.

To further probe which sub-cellular compartments might be affected by interference with Rab5 pathway, we generated and tested a battery of sub-cellular markers. These include (*i*) markers for diverse endosomal compartments such as GNOM<sup>29</sup> (Supplementary Fig. 7a), VPS29<sup>32</sup> (Supplementary Fig. 7b), SNX1<sup>33</sup> (Supplementary Fig. 7c) (*ii*) late endosome/vacuolar marker RabG3f<sup>34</sup> (Supplementary

Fig. 7d); (iii) ER marker NIP1 (Supplementary Fig. 7f); (iv) *cis*-Golgi marker  $\gamma$ -COP<sup>35</sup> (Supplementary Fig. 6h) and (v) Golgi markers such as SYP32<sup>36</sup> (Supplementary Fig. 6b) and GNL1-YFP<sup>37,38</sup> (Supplementary Fig. 6d); (vi) post Golgi markers RabA5d<sup>34</sup> (Supplementary Fig. 6a), RabD2B<sup>39</sup> (Supplementary Fig. 6c), VHAa1<sup>40</sup> (Supplementary Fig. 6e), SYP43<sup>36</sup> (Supplementary Fig. 6f), SCAMP1<sup>41</sup> (Supplementary Fig. 6g) and (vii) vacuolar marker VAMP711<sup>36</sup> (Supplementary Fig. 7e). At 4-8 hours after induction of DN-Ara7 expression, when endocytosis (as monitored by FM4-64 uptake and PIN internalization) is reduced, we detected no visible effects on appearance of these markers, neither we observed significant alterations in their responses to BFA treatment (Supplementary Fig. 6,7) with exception that the number of VPS29- and SNX1-containing compartments is slightly reduced (not shown). These results suggest that interference with Rab5 pathway in *Arabidopsis* primarily affects endocytosis of diverse PM-resident proteins including PINs.

## **Supplementary References**

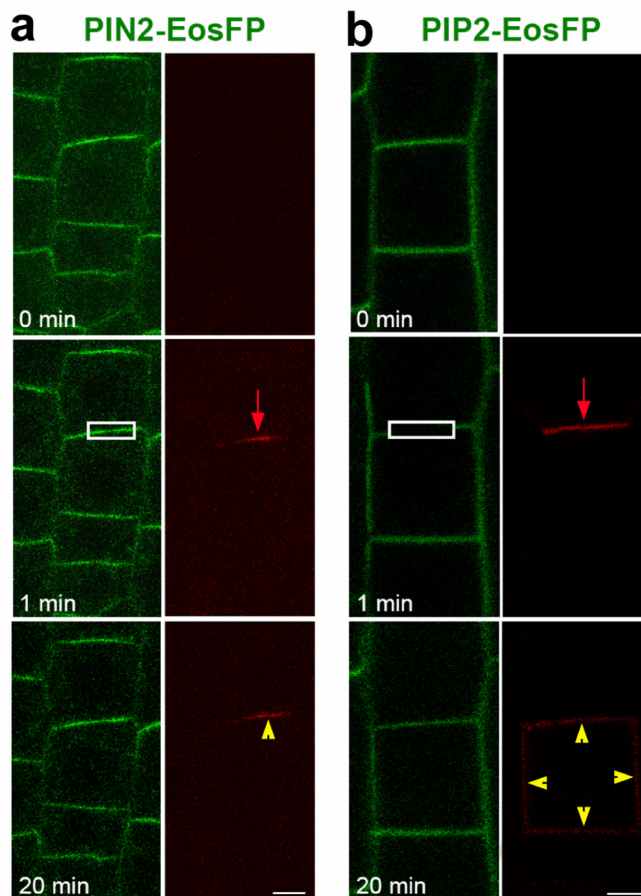
1. Paciorek, T. et al. Auxin inhibits endocytosis and promotes its own efflux from cells. *Nature* **435**, 1251-6 (2005).
2. Friml, J. et al. Efflux-dependent auxin gradients establish the apical-basal axis of *Arabidopsis*. *Nature* **426**, 147-53 (2003).
3. Friml, J. et al. AtPIN4 mediates sink-driven auxin gradients and root patterning in *Arabidopsis*. *Cell* **108**, 661-73 (2002).
4. Blilou, I. et al. The PIN auxin efflux facilitator network controls growth and patterning in *Arabidopsis* roots. *Nature* **433**, 39-44 (2005).
5. Swarup, R. et al. Localization of the auxin permease AUX1 suggests two functionally distinct hormone transport pathways operate in the *Arabidopsis* root apex. *Genes Dev* **15**, 2648-53 (2001).
6. Dubrovsky, J. G. et al. Auxin acts as a local morphogenetic trigger to specify lateral root founder cells. *Proc Natl Acad Sci U S A* **105**, 8790-4 (2008).
7. Haecker, A. et al. Expression dynamics of WOX genes mark cell fate decisions during early embryonic patterning in *Arabidopsis thaliana*. *Development* **131**, 657-68 (2004).

8. Kares, C., Prinsen, E., Van Onckelen, H. & Otten, L. IAA synthesis and root induction with iaa genes under heat shock promoter control. *Plant Mol Biol* **15**, 225-236 (1990).
9. Heisler, M. G. et al. Patterns of auxin transport and gene expression during primordium development revealed by live imaging of the Arabidopsis inflorescence meristem. *Curr Biol* **15**, 1899-911 (2005).
10. Reinhardt, D. et al. Regulation of phyllotaxis by polar auxin transport. *Nature* **426**, 255-60 (2003).
11. Benkova, E. et al. Local, efflux-dependent auxin gradients as a common module for plant organ formation. *Cell* **115**, 591-602 (2003).
12. Sauer, M. et al. Canalization of auxin flow by Aux/IAA-ARF-dependent feedback regulation of PIN polarity. *Genes Dev* **20**, 2902-11 (2006).
13. Scarpella, E., Marcos, D., Friml, J. & Berleth, T. Control of leaf vascular patterning by polar auxin transport. *Genes Dev* **20**, 1015-27 (2006).
14. Bucci, C. et al. The small GTPase rab5 functions as a regulatory factor in the early endocytic pathway. *Cell* **70**, 715-28 (1992).
15. Gorvel, J. P., Chavrier, P., Zerial, M. & Gruenberg, J. rab5 controls early endosome fusion in vitro. *Cell* **64**, 915-25 (1991).
16. McLauchlan, H. et al. A novel role for Rab5-GDI in ligand sequestration into clathrin-coated pits. *Curr Biol* **8**, 34-45 (1998).
17. Sato, M. et al. Caenorhabditis elegans RME-6 is a novel regulator of RAB-5 at the clathrin-coated pit. *Nat Cell Biol* **7**, 559-69 (2005).
18. van der Bliek, A. M. A sixth sense for Rab5. *Nat Cell Biol* **7**, 548-50 (2005).
19. Zerial, M. & McBride, H. Rab proteins as membrane organizers. *Nat Rev Mol Cell Biol* **2**, 107-17 (2001).
20. Vitale, G. et al. The GDP/GTP cycle of Rab5 in the regulation of endocytotic membrane traffic. *Cold Spring Harb Symp Quant Biol* **60**, 211-20 (1995).
21. Horiuchi, H. et al. A novel Rab5 GDP/GTP exchange factor complexed to Rabaptin-5 links nucleotide exchange to effector recruitment and function. *Cell* **90**, 1149-59 (1997).

22. Hass, A. K., Fuchs, E., Kopajtich, R. & Barr, F. A. A GTPase-activating protein controls Rab5 function in endocytic trafficking. *Nat Cell Biol* **7**, 887-93 (2005).
23. Stenmark, H. et al. Inhibition of rab5 GTPase activity stimulates membrane fusion in endocytosis. *Embo J* **13**, 1287-96 (1994).
24. Ueda, T., Uemura, T., Sato, M. H. & Nakano, A. Functional differentiation of endosomes in *Arabidopsis* cells. *Plant J* **40**, 783-9 (2004).
25. Carney, D. S., Davies, B. A. & Horazdovsky, B. F. Vps9 domain-containing proteins: activators of Rab5 GTPases from yeast to neurons. *Trends Cell Biol* **16**, 27-35 (2006).
26. Goh, T. et al. VPS9a, the common activator for two distinct types of Rab5 GTPases, is essential for the development of *Arabidopsis thaliana*. *Plant Cell* **19**, 3504-15 (2007).
27. Dhonukshe, P. et al. Endocytosis of cell surface material mediates cell plate formation during plant cytokinesis. *Dev Cell* **10**, 137-50 (2006).
28. Friml, J. et al. A PINOID-dependent binary switch in apical-basal PIN polar targeting directs auxin efflux. *Science* **306**, 862-5 (2004).
29. Geldner, N. et al. The *Arabidopsis* GNOM ARF-GEF mediates endosomal recycling, auxin transport, and auxin-dependent plant growth. *Cell* **112**, 219-30 (2003).
30. Geldner, N., Friml, J., Stierhof, Y. D., Jurgens, G. & Palme, K. Auxin transport inhibitors block PIN1 cycling and vesicle trafficking. *Nature* **413**, 425-8 (2001).
31. Dhonukshe, P. et al. Clathrin-mediated constitutive endocytosis of PIN auxin efflux carriers in *Arabidopsis*. *Curr Biol* **17**, 520-7 (2007).
32. Jaillais, Y. et al. The retromer protein VPS29 links cell polarity and organ initiation in plants. *Cell* **130**, 1057-70 (2007).
33. Jaillais, Y., Fobis-Loisy, I., Miege, C., Rollin, C. & Gaude, T. AtSNX1 defines an endosome for auxin-carrier trafficking in *Arabidopsis*. *Nature* **443**, 106-9 (2006).
34. Rutherford, S. & Moore, I. The *Arabidopsis* Rab GTPase family: another enigma variation. *Curr Opin Plant Biol* **5**, 518-28 (2002).

35. Movafeghi, A., Happel, N., Pimpl, P., Tai, G. H. & Robinson, D. G. Arabidopsis Sec21p and Sec23p homologs. Probable coat proteins of plant COP-coated vesicles. *Plant Physiol* **119**, 1437-46 (1999).
36. Uemura, T. et al. Systematic analysis of SNARE molecules in Arabidopsis: dissection of the post-Golgi network in plant cells. *Cell Struct Funct* **29**, 49-65 (2004).
37. Richter, S. et al. Functional diversification of closely related ARF-GEFs in protein secretion and recycling. *Nature* **448**, 488-92 (2007).
38. Teh, O. K. & Moore, I. An ARF-GEF acting at the Golgi and in selective endocytosis in polarized plant cells. *Nature* **448**, 493-6 (2007).
39. Batoko, H., Zheng, H. Q., Hawes, C. & Moore, I. A rab1 GTPase is required for transport between the endoplasmic reticulum and golgi apparatus and for normal golgi movement in plants. *Plant Cell* **12**, 2201-18 (2000).
40. Dettmer, J., Hong-Hermesdorf, A., Stierhof, Y. D. & Schumacher, K. Vacuolar H<sup>+</sup>-ATPase activity is required for endocytic and secretory trafficking in Arabidopsis. *Plant Cell* **18**, 715-30 (2006).
41. Lam, S. K. et al. Rice SCAMP1 defines clathrin-coated, trans-golgi-located tubular-vesicular structures as an early endosome in tobacco BY-2 cells. *Plant Cell* **19**, 296-319 (2007).

## Supplementary Figures



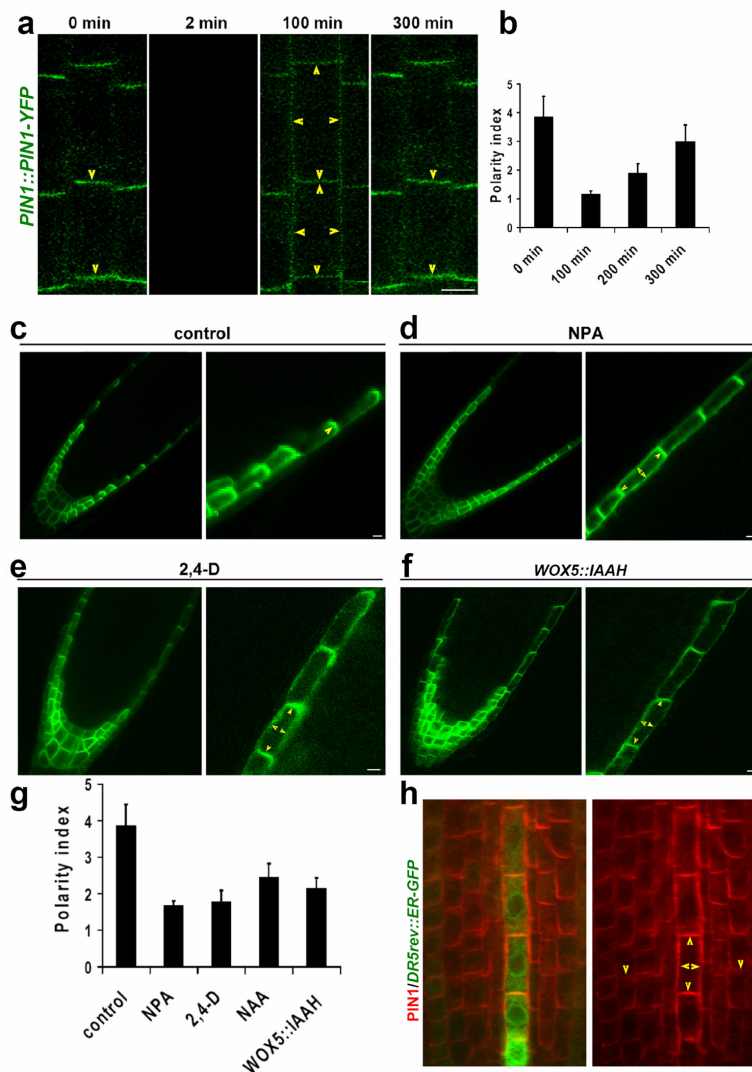
**Supplementary Figure 1 - Lateral PM translocation of PIN2-EosFP and PIP2-EosFP**

(a) Analysis of lateral PM translocation of green-to-red photoconverted PIN2-EosFP (red arrow).

(b) Analysis of lateral PM translocation of green-to-red photoconverted PIP2-EosFP (red arrow).

Note that photoconverted PIN2-EosFP (red coloured) shows much less lateral spreading (yellow arrowhead) within the PM as compared to PIP2-EosFP (red coloured, yellow arrowheads) within the same time frame.

All are root cells. Scale bars are 5  $\mu$ M.



### Supplementary Figure 2 - Auxin effect on PIN polarity

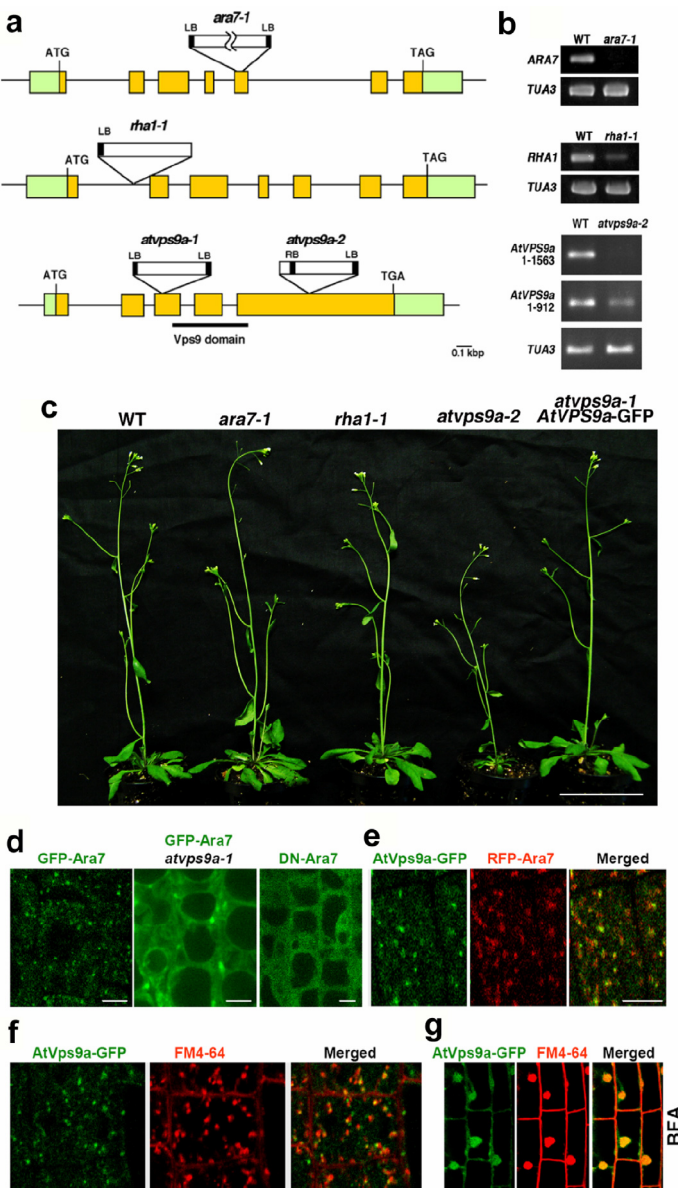
**(a)** Targeting of newly synthesized PIN1-YFP to the PM after its complete photobleaching in presence of auxin (NAA, 25  $\mu$ M). Note PIN1-YFP localization (yellow arrowheads) at the PM in a non-polar manner (3<sup>rd</sup> panel) before becoming polar (4<sup>th</sup> panel). The PIN1 polarity establishment is delayed in presence of auxin as compared to control (see Fig. 1a)

**(b)** Quantitative polarity index (polar to lateral ratio of PIN1-YFP intensity) for FRAP experiments. Bars represent means and error bars are S.D. ( $n=15$ )

**(c-f)** Manipulation of auxin levels with auxin transport inhibitor (NPA 1  $\mu$ M, 12 hr) (d), synthetic auxin (2,4-D 10  $\mu$ M, 2 hr) (e) and by enhancing auxin synthesis in *WOX5::IAAH* plants (grown for 2 hr on plates containing 10  $\mu$ M IAM) (f) and PIN polarity analysis in a polarized lateral root cap cells by expressing PIN2-GFP under the control of auxin-insensitive lateral root-cap specific promoter. Control is shown in c. Note that PIN2-GFP is polar (yellow arrowhead) in control whereas it becomes less polar (yellow arrowheads) following auxin manipulation by all the three methods.

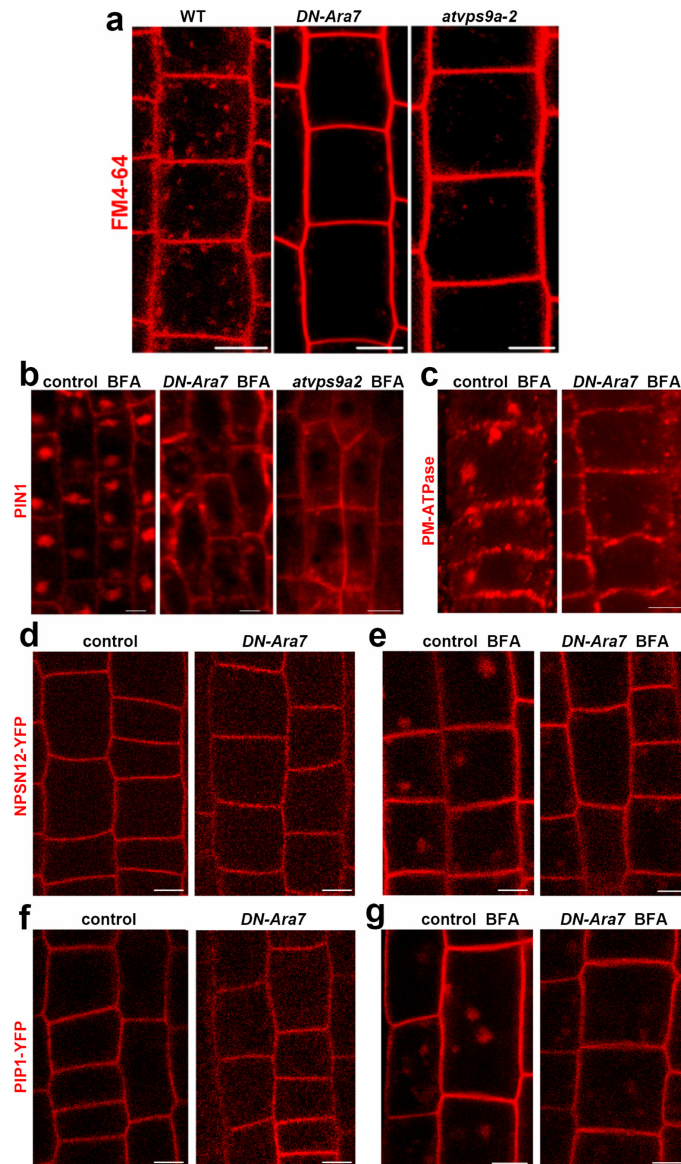
**(g)** Quantitative polarity index shows decrease in PIN2 polarity after manipulation of auxin levels with auxin transport inhibitor NPA (1  $\mu$ M, 12 hr), synthetic auxins 2,4-D (10  $\mu$ M, 2 hr) and NAA (25  $\mu$ M, 2 hr) or by enhancing auxin synthesis in *WOX5::IAAH* plants (grown for 2 hr on plates containing 10  $\mu$ M IAM).

**(h)** Less polar localization (yellow arrowheads) of PIN1 (red) in a cell file with apparently higher auxin levels [inferred from auxin response reporter *DR5rev::ER-GFP* (green)] as compared to other cell files. All are root cells. Scale bars are 5  $\mu$ M.



**Supplementary Figure 3 - *Arabidopsis* Rab5 pathway mutants and localization of Rab5-homologue Ara7 and its GEF AtVps9a**

- (a) Gene structure of *Arabidopsis* Rab5 homologues Ara7 and Rha1 and their activator GEF AtVps9a. The yellow boxes depict exons, and the connecting lines indicate the introns. Light green coloured boxes represent untranslated regions. Locations of T-DNA (white boxes) insertions are shown at respective places.
- (b) RT-PCR showing down regulation of endogenous Ara7, Rha1, AtVps9a transcripts in *ara7-1*, *rha1-1* and *atvps9a-2* mutants. Tubulin 3 (TUA3) expression is used as a control.
- (c) Phenotypes of *ara7-1*, *rha1-1*, *atvps9a-2* and the embryo lethal *atvps9a-1* complemented with functional *AtVps9a*:*AtVps9a-GFP* fusion after inflorescence emergence.
- (d) Sub cellular localization of GFP-Ara7 in wild type and in *atvps9a-1* as compared to the localization of DN-GFP-Ara7. Note the cytosolic distribution of non-functional Ara7 variants.
- (e-f) Colocalization of RFP-Ara7 (e) and endocytic tracer FM4-64 (f) with AtVps9a-GFP in the complemented *atvps9a-1* mutant.
- (g) BFA sensitivity of AtVps9a-GFP labelled endosomal compartment in the presence of FM4-64. Scale bars, in (c) 5 cm and in (d-g) 5  $\mu$ m.

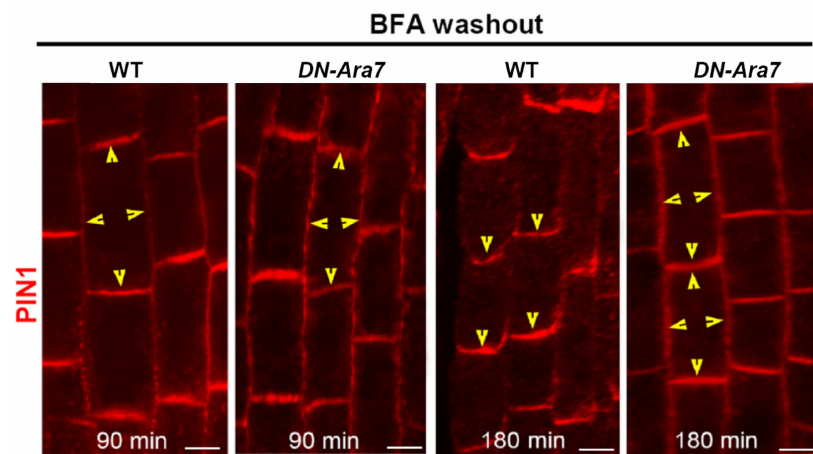


**Supplementary Figure 4. Effect of interference with *Arabidopsis* Rab5 pathway on endocytosis**

(a) Uptake of endocytic tracer FM4-64 (30 min) is reduced following induction of DN-Ara7 expression (4 hr of tamoxifen treatment), and in *atvps9a-2* mutant as compared to wild type.

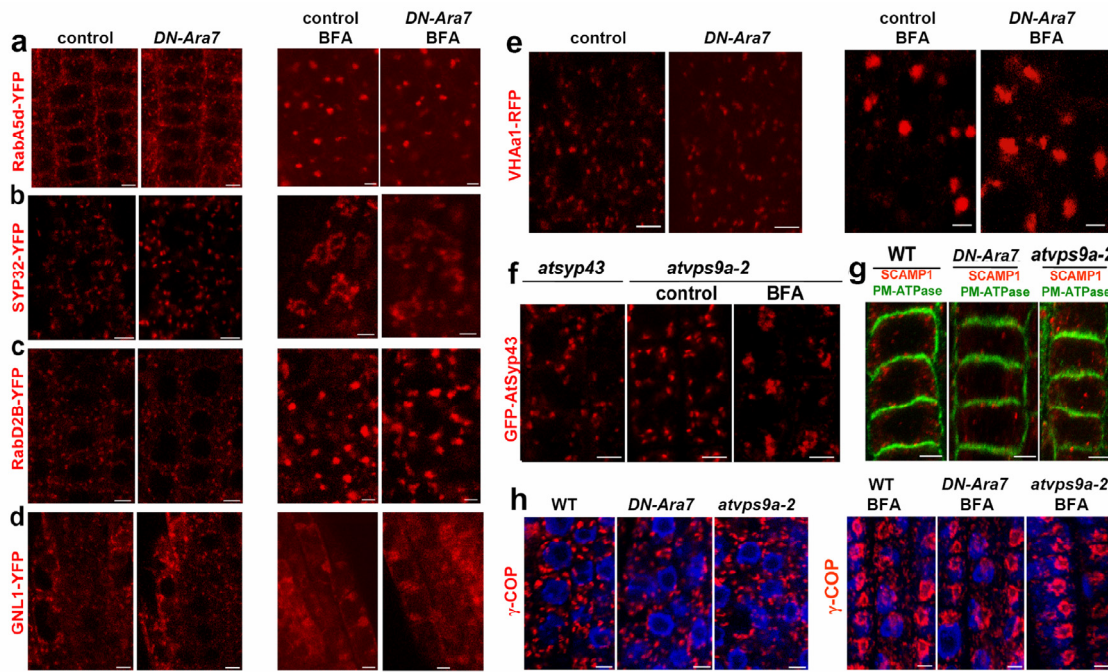
(b, c) Internalization of PIN1 (b) and PM-ATPase (c) (following 90 min of BFA treatment) is reduced following induction of DN-Ara7 expression (4 hr tamoxifen treatment), and in *atvps9a-2* mutant as compared to wild type. Note smaller BFA compartments and more PIN1 (b) and PM-ATPase (c) signal at the PM in *DN-Ara7* and *atvps9a-2*.

(d-g) Comparison of localization of PM markers NSPN12-YFP (d) and PIP1-YFP (f) as well as their response to BFA (90 min treatment) in control and following DN-Ara7 expression (4 hr induction) (e,g). Note that internalization of both NSPN12-YFP and PIP1-YFP is reduced following DN-Ara7 expression. All are root cells. Scale bars are 5  $\mu$ M.

**Supplementary Figure 5 - PIN1 recycling after interference with *Arabidopsis* Rab5 pathway**

Recycling of PIN1 to the PM after BFA washout occurs in both wild type and *DN-Ara7* (3hr tamoxifen treatment). Note that in both cases recycled PIN1 is targeted first to PM in a less polar manner. With time, PIN1 establishes polar localization in the wild type but stays less polar in *DN-Ara7* (6hr tamoxifen treatment).

All are root cells. Scale bars are 5  $\mu$ m.

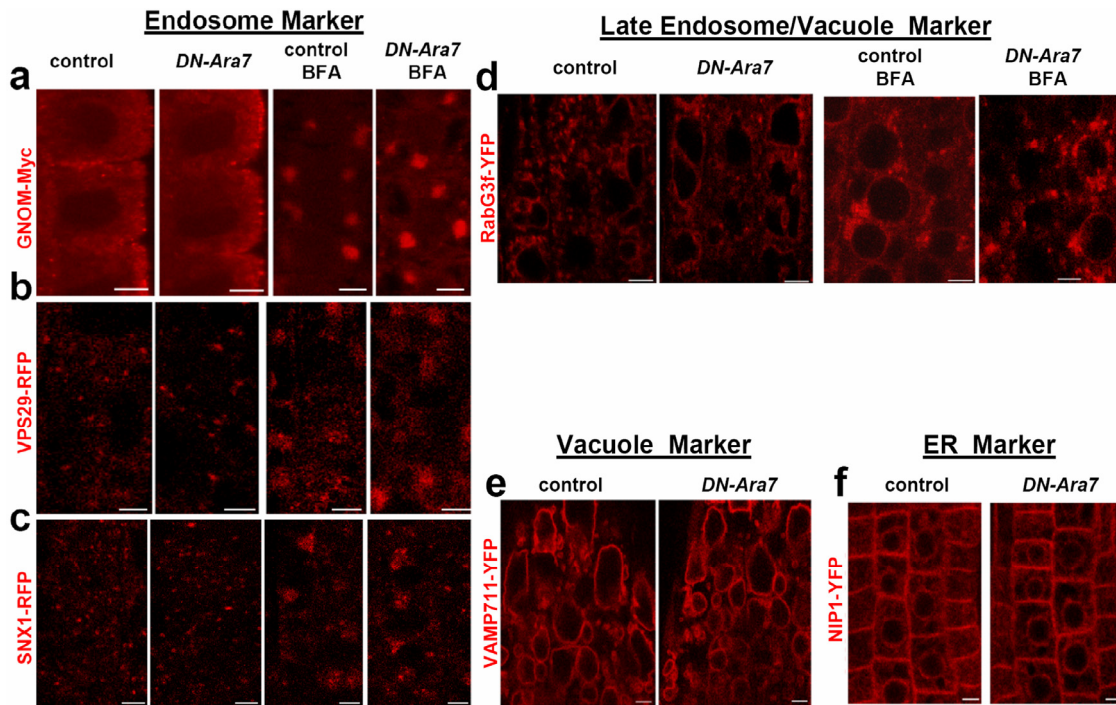


**Supplementary Figure 6 - Interference with *Arabidopsis* Rab5 endocytic pathway does not strongly affect Golgi and Post-Golgi markers**

- (a) Comparison of TGN/post Golgi marker RabA5d-YFP and its response to BFA (90 min treatment) in control and following *DN-Ara7* expression (4 hr induction).
- (b) Comparison of Golgi marker SYP32-YFP and its response to BFA (90 min treatment) in control and following *DN-Ara7* expression (4 hr induction).
- (c) Comparison of Golgi marker RabD2b-YFP and its response to BFA (90 min treatment) in control and following *DN-Ara7* expression (4 hr induction).
- (d) Comparison of Golgi marker GNOM Like 1 (GNL1)-YFP and its response to BFA (90 min treatment) in control and following *DN-Ara7* expression (4 hr induction).
- (e) Comparison of TGN marker VHAa1-RFP and its response to BFA (90 min treatment) in control and following *DN-Ara7* expression (4 hr induction).
- (f) Comparison of TGN marker GFP-AtSyp43 in *atvps9a-2* mutant and in *atvps9a-2* mutant and response of GFP-AtSyp43 labelled TGN to BFA (90 min treatment) in *atvps9a-2* mutant.
- (g) Comparison of TGN marker SCAMP1 and PM marker PM-ATPase in wild-type, following *DN-Ara7* expression (4 hr induction) and in *atvps9a-2* mutant.
- (h) Comparison of *cis*-Golgi marker  $\gamma$ -COP and its response to BFA (90 min treatment) in wild type, following *DN-Ara7* expression (4 hr induction) and in *atvps9a-2* mutant.

Note that none of the tested Golgi-Post Golgi markers show noticeable changes following *DN-Ara7* expression and in *atvps9a-2* mutant.

All are root cells. Scale bars are 5  $\mu$ M.

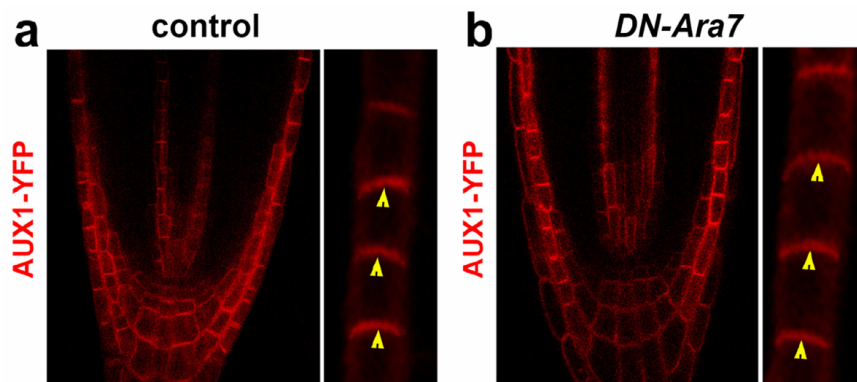


**Supplementary Figure 7 - Interference with *Arabidopsis* Rab5 endocytic pathway does not strongly affect endosomal, vacuolar and endoplasmic reticulum (ER) markers**

- (a) Comparison of recycling endosomal marker GNOM-Myc and its response to BFA (90 min treatment) in control and following DN-Ara7 expression (4 hr induction).
- (b) Comparison of retromer marker VPS29-RFP and its response to BFA (90 min treatment) in control and following DN-Ara7 expression (4 hr induction).
- (c) Comparison of sorting endosomal marker SNX1-RFP and its response to BFA (90 min treatment) in control and following DN-Ara7 expression (4 hr induction).
- (d) Comparison of late endosome/vacuolar marker RabG3f and its response to BFA (90 min treatment) in control and following DN-Ara7 expression (4 hr induction).
- (e) Comparison of vacuolar marker VAMP711-YFP in control and following DN-Ara7 expression (4 hr induction).
- (f) Comparison of localization of ER-marker NIP1-YFP in control and following DN-Ara7 expression (4 hr induction)

Note that the tested endosomal and vacuolar markers are not visibly affected following DN-Ara7 expression.

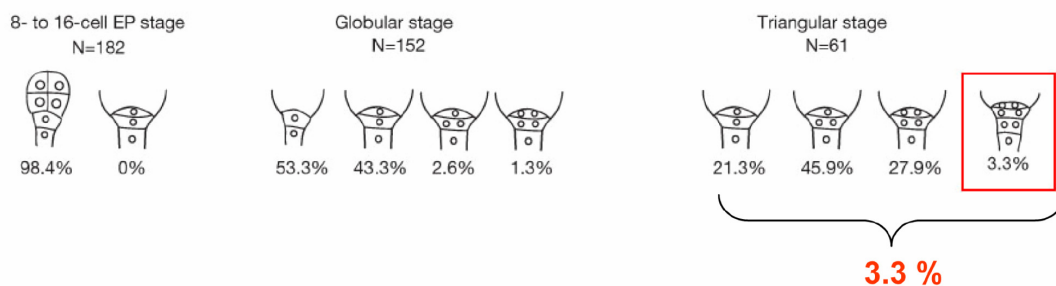
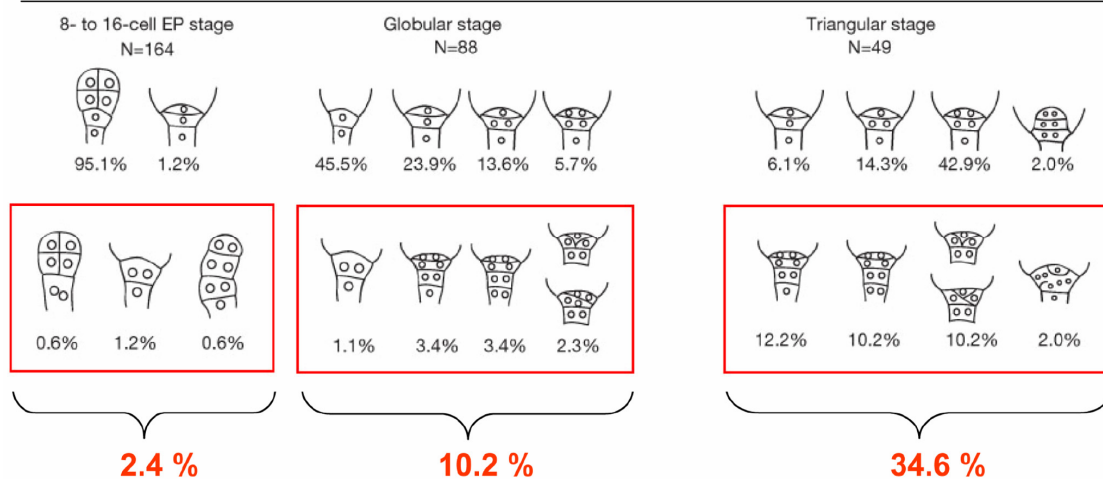
All are root cells. Scale bars are 5  $\mu$ M.



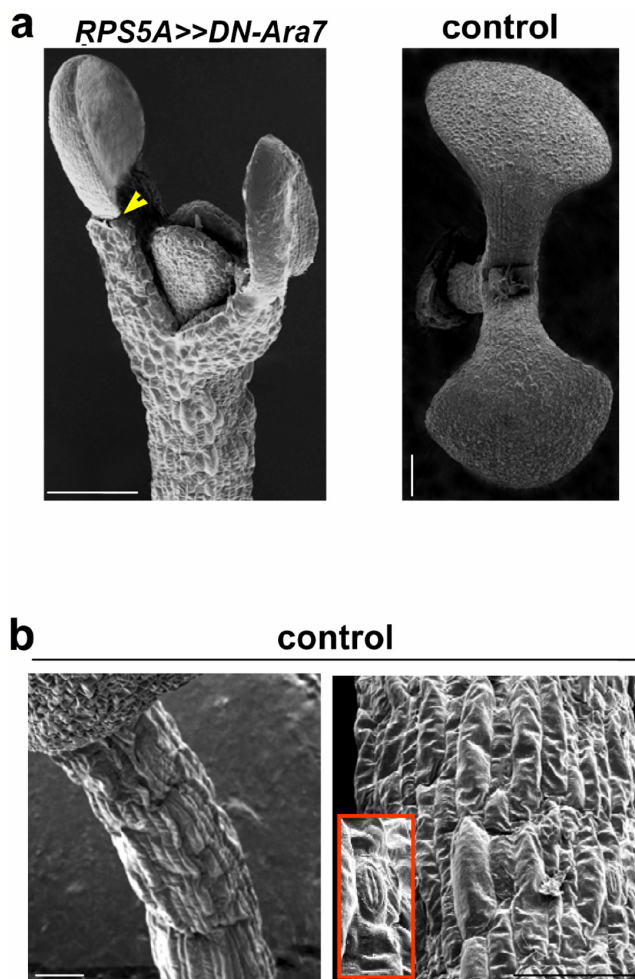
**Supplementary Figure 8 - Effect of DN-Ara7 expression-mediated endocytic impairment on polar localization of AUX1 (auxin influx carrier)-YFP.**

(a, b) Note that AUX1-YFP remains largely apical (yellow arrowheads) in protophloem cells following DN-Ara7 expression (4 hr, b) similar to its localization in control (a).

All are root cells. Scale bars are 5  $\mu$ M.

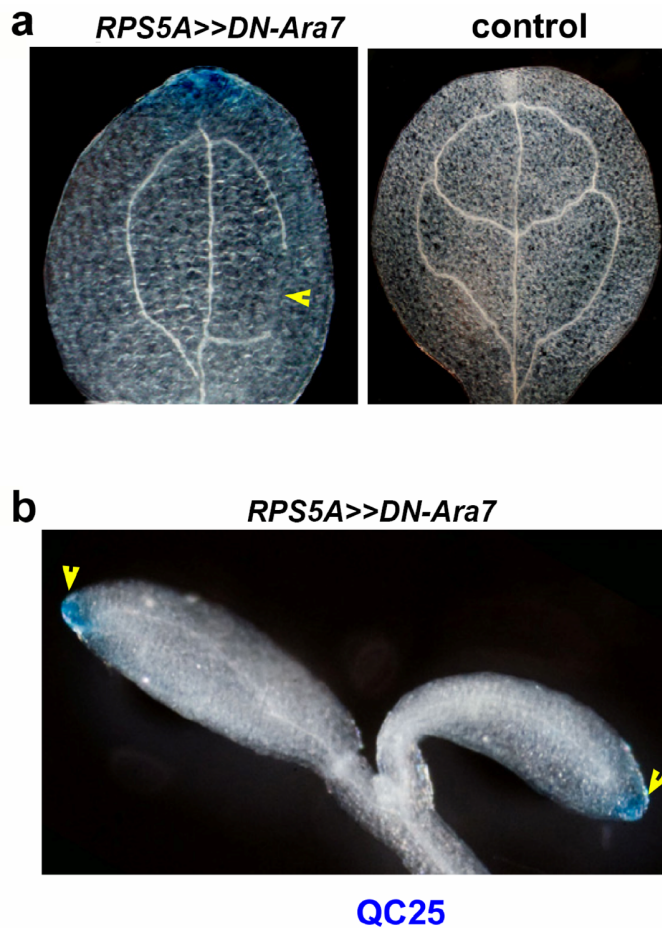
**RPS5A control****RPS5A>>DN-Ara7**

**Supplementary Figure 9 - Comparison and frequencies of distinct categories of root pole phenotypes in control and *RPS5A>>DN-Ara7* embryos at different stages of embryogenesis**



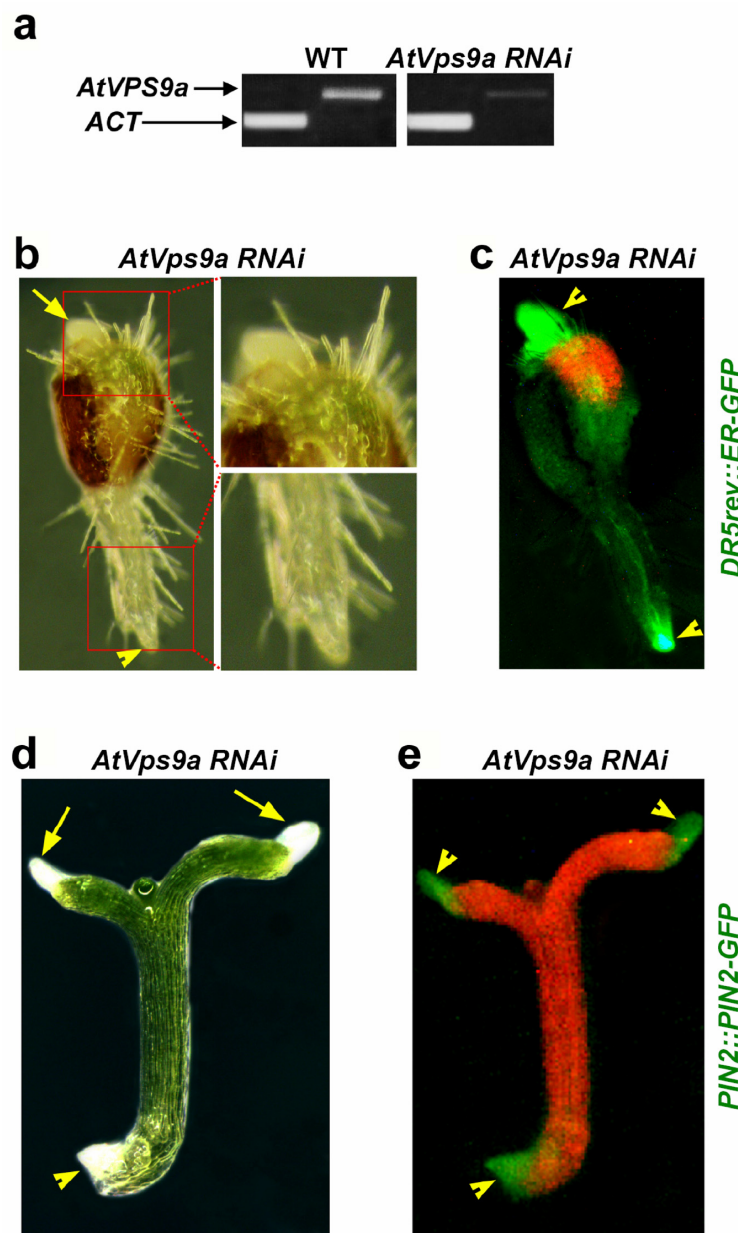
**Supplementary Figure 10 - SEM analysis of control and *RPS5A>>DN-Ara7* seedlings**

(a) Note the root-like structures emerging from the cotyledons of *RPS5A>>DN-Ara7* seedlings display different morphological features as compared to control cotyledons. Yellow arrowhead depicts the boundary between the root-like structure and cotyledon part.  
(b) SEM of hypocotyl. Note that hypocotyl also bears few stomata (red inset) those are completely absent on the cotyledon-originated root-like structure (see Fig. 4c, d).  
Scale bars, in (a) 250  $\mu$ m and in (b) 100  $\mu$ m.



**Supplementary Figure 11 - Vascular defects and root-specific marker expression in cotyledons of *RPS5A>>DN-Ara7***

- (a) Note the incomplete vasculature (an auxin transport defect-related phenotype) in cotyledon of *RPS5A>>DN-Ara7* seedling as compared to the normal complete vasculature in control cotyledon.
- (b) Expression of root-specific QC marker QC25-GUS at the tips of the *RPS5A>>DN-Ara7* expressing cotyledon.



**Supplementary Figure 12 - Analysis of *AtVps9a RNAi* seedling development**

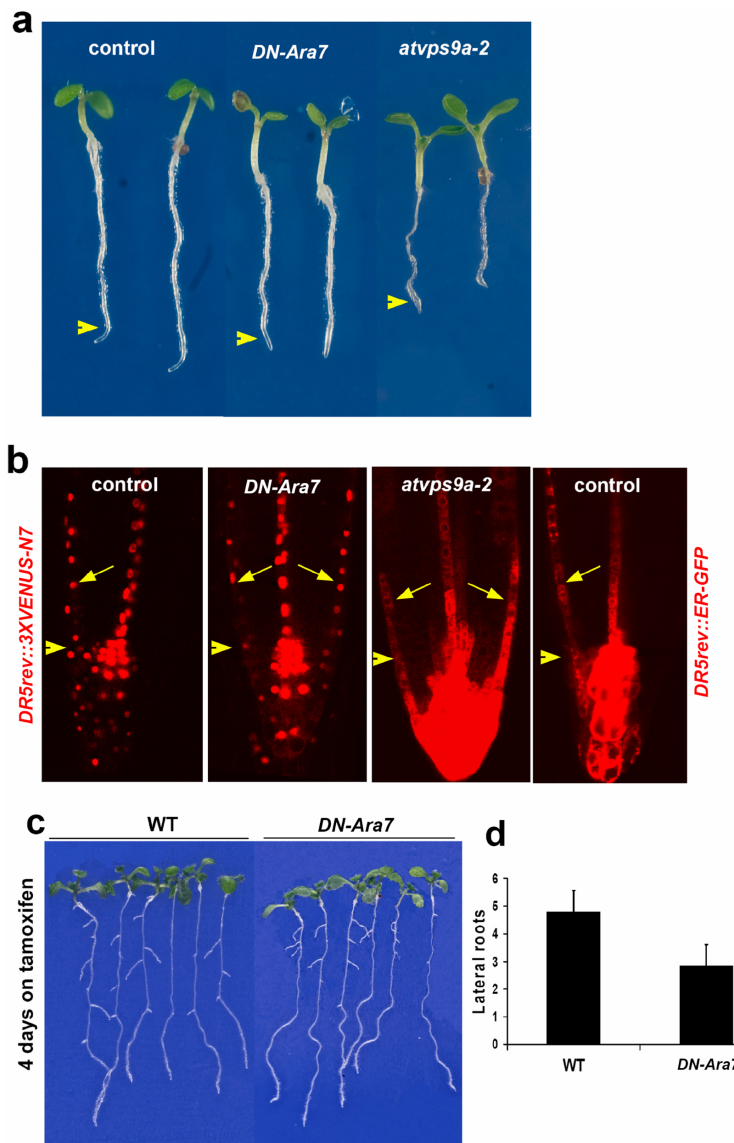
(a) RT-PCR analysis showing reduced expression of AtVps9a in *AtVps9aRNAi* as compared to its expression in the wild type. Actin expression is used as a control.

(b) Root-like structure (yellow arrow) emerging from the apical part in *AtVps9aRNAi* line. Note that the apical region shows root hairs (root-specific epidermal structures) similar those present on a main root. Main root is shown by yellow arrowhead.

(c) Auxin response maxima visualized by *DR5rev::ER-GFP* in *AtVps9aRNAi* line. Note that in addition to the tip of the main root (where normally the auxin response maxima is detected) the apical root-like structure also bears auxin response maxima (see upper and lower yellow arrowheads).

(d) Root-like structures (yellow arrows) emerging from the cotyledon in *AtVps9aRNAi* line. Main root is shown by yellow arrowhead.

(e) Expression of a root-specific *PIN2-GFP* (yellow arrowheads) in both the root-like structures emerging from the cotyledons and in the rudimentary main root of *AtVps9aRNAi* line.



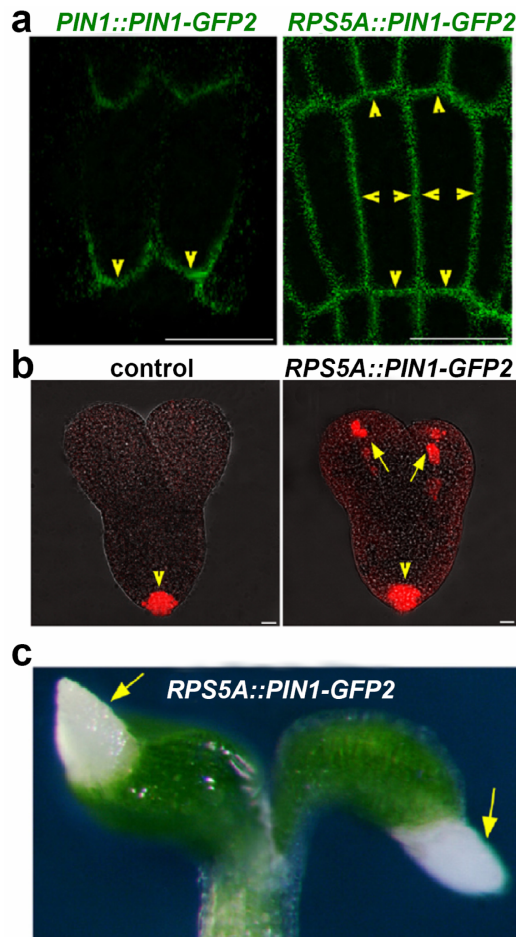
**Supplementary Figure 13 - Interference with *Arabidopsis* Rab5 endocytic pathway affects gravitropism and lateral root formation**

(a) Gravity-induced root tip curvature in control, following *DN-Ara7* expression and in *atvps9a-2* mutant. Note that seedlings expressing *DN-Ara7* (induced for 4 hr before gravity impulse and induction continued during gravity perception) and those that are mutant for *atvps9a-2* largely fail to effectively respond to gravity impulse. Position of the root tip at the moment of gravity stimulation is indicated by yellow arrowheads.

(b) Gravity impulse-mediated asymmetric *DR5rev::3XVENUS-N7* and *DR5rev::ER-GFP* distribution (yellow arrows) towards the lower side of the roots (yellow arrowheads) in controls. No asymmetric distribution (yellow arrows) of *DR5rev::3XVENUS-N7* (following *DN-Ara7* expression) and *DR5rev::ER-GFP* (in *atvps9a-2* mutant) after gravity impulse. Lower side of gravity-stimulated roots is shown by yellow arrowheads.

(c) Comparison of lateral root formation in control and following *DN-Ara7* expression in 8 days old seedlings (both kept on tamoxifen plates for 4 days after shifting from control plates at 4 days post-germination).

(d) Quantification of total number of lateral roots. Note that seedlings expressing *DN-Ara7* produce less lateral roots as compared to the control.



**Supplementary Figure 14 - Effect of expression of non-polar PIN1 variant on auxin distribution and development**

(a) *RPS5A::PIN1-GFP2* expressing embryos show largely non-polar PIN1-GFP2 localization as compared to the control.

(b) Altered auxin response (visualized by *DR5rev::3XVENUS-N7*) in *RPS5A::PIN1-GFP2* expressing heart-shaped embryos. Note pronounced DR5 auxin response maxima (yellow arrowhead) at the root pole in control and *RPS5A::PIN1-GFP2* embryos and additional larger DR5 maxima in embryonic leaves (yellow arrows) of *RPS5A::PIN1-GFP2* embryos.

(c) *pin1-/-,2,3,4,7-/+* seedlings expressing *RPS5A::PIN1-GFP2* show root-like structures emerging from cotyledons similar to those observed in *RPS5A>>DN-Ara7* and in *AtVps9aRNAi* (shown in Figure 4a)

**Supplementary Table 1: Primer Sequences used for cloning and genotyping**

Primer Name	Sequence
Syp43-f	GCCTTCGTTGGGGATGGTA
Syp43-r	CAAGAACAGACGCACACATC
LB	GACCGCTTGCTGCAACTCTCTCA
Ara7-f	CCTGCGATTCTCTTCAGATCGATA
Ara7-r	GCTATTACACACACATAGCTAAC
Rha1-f	TCTCGAGCTTCAAATACTGTTCAGA
Rha1-r	CTAAGCACAAACACGATGAA
DS-Lox	AACGTCCGCAATGTGTTATTAAGTTGTC
AtVps9a-f	ATGGAGAACACGGACGTCTCTTGG
AtVps9a-r	TCACTCAGAACGCTCCGTAACTGG
ACT-f	GCCGATGAAGCTCAATCCAAA
ACT-r	GGTCACGACCAGCAAGATCAAG
DN-Ara7-f	TTGGTGCTGGAAAAAAATAGTCTTGTACGG
DN-Ara7-r	CCGTAACACAAGACTATTTTCCAGCACCAAC
pin1F-attB1	GGGGACAAGTTGTACAAAAAAGCAGGCTAAATGATTACGGC
	GGCGGACTTCT
pin1R-attB2	GGGGACCACTTGTACAAGAAAGCTGGGTCTCATAGACCCAA
	GAGAATGTAGTAGAGAAAG
pAtRPS5A-F	GGGGACAACCTTGTATAGAAAAGTTGTACCGGGCCATAAT
	CGTGAGTAG
pAtRPS5A-R	GGGGACTGCTTTGTACAAACTGTCCGGCTGTGGTGAGAG
	AAACAGAGCG
At1g79580-PF-ApaI	GGGCCCTCGTTGAAGATGCCTGGATTAAATACTG
At1g79580-PR-BamHI	GGGATCCTTACTCTTAAAGCAAAC